Vol. 21, No. 1, Spring, 2025, 57-72
DOI: 10.22055/ivj.2025.482863.2744
Journal Homepage: http://www.ivj.ir/ ***Original Article***

Morphologic and morphometric study of the lumbosacral vertebrae in guinea pig (*Cavia porcellus*) based on CT scan images

Elaheh Goli[1], Siamak Alizadeh[2*] and Mohammadreza Hosseinchi[3]

[1] DVM Graduate, Faculty of Veterinary Medicine, Ur. C., Islamic Azad University, Urmia, Iran
[2] Assistant Professor, Department of Clinical Sciences, Faculty of Veterinary Medicine, Nag. C., Islamic Azad University, Naghadeh, Iran
[3] Assistant Professor, Department of Basic Sciences, Faculty of Veterinary Medicine, Ur. C., Islamic Azad University, Urmia, Iran

Received: 11.10.2024 Accepted: 14.04.2025

Abstract

Computed tomography (CT) is an accurate diagnostic imaging technique used to evaluate the vertebral column in exotic and small animals. The present study aimed to investigate the morphology and morphometric of the normal lumbosacral vertebrae in guinea pigs (Cavia porcellus) using CT scan images. This cross-sectional descriptive study utilized 10 healthy adult guinea pigs (*Cavia Porcellus*) (5 males and 5 females) with a mean age of 12 ± 1.20 months and an average weight of 1.04 ± 0.15 kg. Following anesthetization with a cocktail of xylazine (4 mg/kg) and ketamine (60 mg/kg), CT scans of the lumbosacral vertebrae were performed in the sagittal, transverse, and dorsal planes, from the cranial part of the first lumbar vertebra to the caudal extremity of the sacrum. Based on the results of this study, all parts of the lumbosacral vertebrae and intervertebral joints of guinea pig (*Cavia porcellus*) can be observed and evaluated in computed tomography images. The spinous process of the lumbar vertebrae in the sagittal plane and the cranial and caudal articular processes in the sagittal and transverse reconstruction planes were more identifiable. The mammillary processes and the cranial and caudal vertebral notches were better observed in the dorsal plan. Two lateral recesses were visible in the caudal vertebral foramina of L_6 at the junction of the pedicle and the vertebral body, a feature reported here for the first time. The interarcuate spaces of guinea pig lumbar vertebrae were very narrow, but this space was wide and large between the L_6 and S_1 vertebrae. For epidural anesthesia, surgeons can perform cerebrospinal fluid puncture and anesthetic drugs injection from this location. In this study, morphometric measurements of different parts of the lumbosacral vertebrae were subjected to statistical analysis. The results of this research can be employed in teaching computed tomographic anatomy of lumbosacral vertebrae, interpretation of CT scan images, as well as in clinical and treatment decisions of guinea pig (*Cavia porcellus*).

Key words: Computed tomography, Guinea pig (*Cavia porcellus*), Lumbosacral vertebrae, Morphology, Morphometric

Introduction

Guinea pigs are mammals from the order of rodents and the family of *Caviidae*. Currently, 13 species of these rodents have been identified. The most common breeds are the American, Abyssinian and Peruvian (Pignon and Mayer, 2020). All types of guinea pigs are social animals and tend to live in groups. Domestic species of guinea pigs (*Cavia porcellus*) are not found in nature (Zipser et al, 2014). This rodent is considered as a popular pet as well as a valuable laboratory animal. The guinea pig

* **Corresponding Author**: Siamak Alizadeh, Assistant Professor, Department of Clinical Sciences, Faculty of Veterinary Medicine, Nag. C., Islamic Azad University, Naghadeh, Iran
E-mail: si.alizadeh@iau.ac.ir

© 2020 by the authors. Licensee SCU, Ahvaz, Iran. This article is an open access article distributed under the terms and conditions of the Creative Commons Attribution-NonCommercial 4.0 International (CC BY-NC 4.0 license) (http://creativecommons.org/licenses/by-nc/4.0/).

was the first animal used in medical research, and its name is synonymous with the experimental animal (Mähler et al, 2014).

The skeleton of the guinea pig is almost entirely bony, divided into axial and appendicular portions. The axial skeleton comprises the skull, vertebral column, ribs, and sternum, while the appendicular skeleton consists of the limbs and limb girdles. The vertebral column is composed of approximately thirty-seven vertebrae, which are separated from one another by intervertebral discs. The guinea pig (*Cavia porcellus*) has 7 cervical, 13 thoracic, 6 lumbar, 4 sacral and 5-7 caudal vertebrae (Barbera et al., 2019). A typical vertebra consists of a body, an arch and processes. The vertebral arch comprises of right and left pedicles and laminae which form the lateral walls and roof of the vertebral canal. Vertebrae are connected to each other through intervertebral joints which are of the diarthrodial type and do not contain joint fluid (Moarabi et al, 2024).

The lumbosacral vertebrae of guinea pigs (*Cavia porcellus*) are among the most complex vertebrae in the spine due to their multiple functions. Complications that may be observed include dysplasia, spondylosis, herniation and mineralization of the intervertebral disc, spinal canal stenosis, fracture, luxation, arthrosis, arthritis and neoplasia (Proks et al, 2021; Shomer et al, 2015). These vertebrae may have complications such as the hemivertebrae, wedge vertebrae, symmetrical hypoplasia, transitional and butterfly vertebrae, spina bifida, herniation and mineralization of the intervertebral disc, spinal canal stenosis, fracture, luxation, arthrosis, arthritis and neoplasias (Segal et al, 2018; Munif et al, 2023).

Various imaging techniques can be useful in diagnosing these injuries. DaCosta and Samii (2010) reported that CT can be a suitable method for evaluating spinal diseases in exotic and small animals. Additionally, CT is preferable to myelography because it is a non-invasive method. Furthermore, they have stated that although the diagnostic sensitivity of MRI is higher than CT, this method cannot be used in cases such as injuries caused by gunshots to the vertebral column. Therefore, in such cases, CT scan will be considered as a suitable selection method (Da Costa and Samii, 2010).

Witkowska et al, (2014), by examining the micro-computed tomography (micro CT) of guinea pig bones, have described some of its bone characteristics and species differences. Proks et al, (2021), by conducting a radioanatomical study on the vertebral column of 240 guinea pigs, stated that 12.5% of them had congenital anomalies related to the vertebral column, with the cervical and lumbosacral vertebrae having the least and the most complications, respectively. In a study, Soroori et al, (2022) reported that there was no significant difference in the height of the extremity plate of lumbar and coccyx vertebrae based on a morphometric evaluation of rabbit lumbosacral vertebrae using the CT method. However, other parameters such as height of the vertebral body and spinous process, length of transverse process and vertebral body were significantly different. Furthermore, they stated that the depth of the spinal canal was uniform from the first lumbar vertebra to the third sacral bone, decreased in the fourth sacral vertebra and remained constant until the second coccygeal vertebra.

McDougall et al, (2009) investigated the relationship between back pain and pathology of intervertebral discs by performing micro-CT of the vertebral column of young (2-5 months) and old (17-37 months) guinea pigs. According to the study, micro CT findings are consistent with histopathology results, and the clinical symptom of pain is a poor predictor for evaluating the degree of degeneration and damage of vertebrae and intervertebral discs. In this context, micro CT indications have greater diagnostic accuracy. Since the guinea pig (*Cavia porcellus*) is used in a wide range of biomedical research, it is necessary to have accurate knowledge of its tissues. The computed tomography images of different tissues of guinea pig can provide valuable information to researchers (Carrera et al, 2022; Wills et al, 2021). Assessment of the tomographic features of the lumbosacral vertebrae of guinea pig (*Cavia porcellus*) can be beneficial in identifying anatomical characteristics and conducting pathological examinations. Therefore, it is necessary to accurately evaluate the normal anatomical, morphological and morphometric details of these vertebrae.

The accurate anatomical information is essential for safe intervention in the rodent lumbosacral region, and knowledge of the morphometry of this region will help reduce surgical risks and complications. Since the surgical techniques of the vertebral column in guinea pigs and/or rodents involve the utilization of bony anatomical landmarks, the morphometric data of the various parts of the vertebrae are essential (Pignon and Mayer, 2020). The precise anatomical dimensional knowledge is important to understand the etiopathogenesis of the complications and disorders of the lumbosacral region (Liau et al, 2017). The bony landmarks like the transverse and spinous processes, body length and height are important during the internal fixation of the lumbar spine (Sun et al, 2022). The anatomical studies help in understanding the detail complex morphometric of the vertebral column. There is an assumption that the morphometry of the vertebrae play a role in degenerative diseases of the vertebral column. The measurements are essential while choosing a suitable implant and this may avoid the intervertebral space exceeding and subsequent injury of the blood vessels. In addition, these studies provide necessary information to designers and manufacturers of spinal devices (Martz et al, 1997). Also, complications such as hemivertebrae, wedge-shaped vertebrae, symmetrical hypoplasia, butterfly vertebrae, transitional vertebrae, and hypoplasia/aplasia of the caudal articular process can cause mild to severe deformity of the lumbosacral vertebrae of the guinea pig. Sometimes, these mild deformities are difficult to detect in the lumbosacral vertebrae (Proks et al, 2015). In order to reach a definite diagnosis, it is necessary to have a normal range of the sizes of these vertebrae to compare suspicious cases with them.

Currently, radioanatomical studies of the lumbosacral vertebrae of guinea pigs (*Cavia porcellus*) are limited and there are no documented and detailed reports in this field. Therefore, this specific study was conducted on these vertebrae, investigating and determining their different parts and normal values.

Material and methods

Study design and animals

This cross-sectional descriptive study utilized 10 healthy adult guinea pigs (*Cavia Porcellus*) (5 males and 5 females). The mean weights of males and females were 1147±80 and 921±58 grams, with average ages of 12±1.01 and 12±0.94 months, respectively. Throughout the study, these animals received proper nutrition and were kept in an isolated room with a temperature of 25°C, relative humidity of 65%, and a 12-hour light/dark cycle (Pignon and Mayer, 2020).

Anesthesia of guinea pigs

The guinea pigs used in the study were placed under general anesthesia using dissociative agents. For this purpose, a combination of Xylazine Hcl (4 mg/kg, IM, Xylamax® 2% injectable, Royan, Iran) and Ketamin Hcl (60 mg/kg, IM, Ketasol® 10% injectable, Alfasan, Holland) was administered intramuscularly (Mitrović et al, 2023).

Computed tomography study

To obtain the CT images, each guinea pig was placed on the CT scanner in a *sternal* recumbent position with its hindlimbs fully extended toward the caudal side. The CT scan of the lumbosacral vertebrae was performed in the sagittal, transverse, and dorsal planes with a thickness and intervals of 1mm from the cranial part of the first lumbar vertebra to the caudal extremity of the sacrum. A helical scanner (Toshiba Multi-slice CT Scanner Asteion Premium 4, Model: TSX-021B, Japan) was employed for the CT imaging. Appropriate windows were selected to examine both soft and bone tissues. The technical factors of the CT scanner included gantry rotation time (400 ms), slice thickness (1 mm), reconstruction distance (0.5–1 mm), pitch ratio (1), kVp (120), mAs (22), physical detector collimation (32 × 0.6 mm), final section collimation (64 × 0.6 mm), resolution (512 × 512 pixels), and resolution range (0.92 × 0.92), Kernel (10 H), and increment (0.5 mm) (Ohlerth and Scharf, 2007; Badea, 2018). Imaging was performed based on the above-mentioned factors, and the obtained images were saved in DICOM format (Witkowska et al, 2014; Bouxsein et al, 2010).

Three-dimensional reconstruction

Following the saving of the obtained images in DICOM format, they were transferred to a computer equipped with 3D modeling software (Onis CT software, Multi-Modality Workplace: VE 2.5A) (Wilhite and Wölfel, 2019). These images were analyzed using the bone (WW: 4000 HU; WL: 550 HU) and soft tissue (WW: 450 HU; WL: 80 HU) settings. The electronic caliper of this software was used for the morphometric measurements.

Morphometric study

The morphometric measurements of different parts of lumbosacral vertebrae were performed and their means were recorded. The measurements were conducted once by the same individual. The NAV (Nomina Anatomica Veterinaria) was used as the obtained scientific term (Veterinaria, 2017; Özkadif et al, 2015). The investigated parameters are listed in Table 1 (Boonsri et al, 2021; De Silva et al, 2022).

Statistical analysis

The SPSS software version 21 was utilized in this trial. Statistical analysis of Student *t*-test was conducted, and the results were presented as Mean±SD. The Confidence Interval (CI) index was employed to calculate the normal ranges of the indices of the lumbosacral vertebrae in the adult guinea pigs. The significance level was set at 0.05.

Table 1: Description of the investigated parameters

Parameter	Abbreviation	Description
Body length	BL	Distance between the cranial articular surfaces to caudal articular surface in sagittal plan.
Articular processes distance	APD	Distance between the cranial articular processes to caudal articular process in sagittal plan.
Arch borders distance	AD	Distance between the cranial and caudal borders of vertebral in sagittal plan.
Total height	TH	Distance between the ventral crest to distal extremity of spinous process of vertebral in sagittal plan.
Body height	BH	Distance between the ventral crest to vertebral foramen in transverse plan.
Spinous process height	SPH	Distance between proximal and distal extremity of spinous in transverse plan.
Vertical diameter of cranial foramen	VDCrF	Distance between proximal extremities of cranial foramen to distal extremity of cranial foramen in transverse plan.
Horizontal diameter of cranial foramen	HDCrF	Distance between left extremities of cranial foramen to right extremity of cranial foramen in transverse plan.
Vertical diameter of caudal foramen	VDCaF	Distance between proximal extremities of caudal foramen to distal extremity of caudal foramen in transverse plan.
Horizontal diameter of caudal foramen	HDCaF	Distance between left extremities of caudal foramen to right extremity of caudal foramen in transverse plan.
Body cranial width	BCrW	Distance between left extremities of cranial body to right extremity of cranial body in transverse plan.
Body caudal width	BCaW	Distance between left extremities of caudal body to right extremity of caudal body in transverse plan.
Lateral sacral crest length	LSL	The craniocaudal length of lateral sacral crest in transverse plan.
Medial sacral crest length	MSL	The craniocaudal length of medial sacral crest in transverse plan.

Results

Based on the results of this study, all guinea pigs under study had 6 lumbar vertebrae with an irregular trapezoidal shape. Each lumbar vertebra was composed of an arch, body, cranial and caudal articular processes, mammillary processes, spinous process and cranial and caudal vertebral notches. The details of joints between transverse and mammillary processes, intervertebral discs and cranial and caudal articular processes could be evaluated in the CT images. All parts of the lumbosacral vertebrae and intervertebral joints of guinea pig (*Cavia porcellus*) can be observed and evaluated in the computed tomography images. The spinous process of the lumbar vertebrae in the sagittal plane and the cranial and caudal articular processes in the sagittal and transverse reconstruction planes were more identifiable. The mammillary processes and the cranial and caudal vertebral notches were better observed in the dorsal plan. The costal facets were not observed in these vertebrae. The spinous processes of the lumbar vertebrae were short and inclined towards the cranial side. The height of the spinous processes from L_1 to L_6 vertebrae decreased gradually. The transverse processes of the lumbar vertebrae were short and flat, located craniolaterally and somewhat ventrally. These processes were articulated with mammillary processes from their proximal part. The L_1 and L_3 vertebrae had the shortest and longest transverse processes, respectively. The lengths of these processes were almost equal in other vertebrae. The articular surfaces of the cranial and caudal extremities of the lumbar vertebrae were smooth. The body length of the L_3 vertebra was longer than other lumbar vertebrae in male and female guinea pigs. The L_4

vertebra had the greatest height and depth of the spinal canal. At the junction of the pedicle with the vertebral body (in the L_6 caudal vertebral foramina), two lateral recesses were visible. The arches of the lumbar vertebrae provided a relatively wide canal for the spinal cord. The intervertebral foramina of the lumbar vertebrae were narrow, but the intervertebral foramen of the last lumbar and the first sacral vertebra were wide. The diameter of intervertebral notches L_1 and L_2 was narrow but it gradually increased up to the L_6 vertebra. The accessory processes (*Anapophysis*) were observed in all lumbar vertebrae, located between the transverse and caudal articular processes. The *anapophysis* of both the first and second lumbar vertebrae of the guinea pig was relatively prominent. The cranial articular processes were visible as two rounded facets on the sides of the vertebral arch, and the caudal articular processes were visible as two facets at the root of the spinous processes. The caudal articular processes facets of the sixth lumbar vertebra were completely separated (Figure 1).

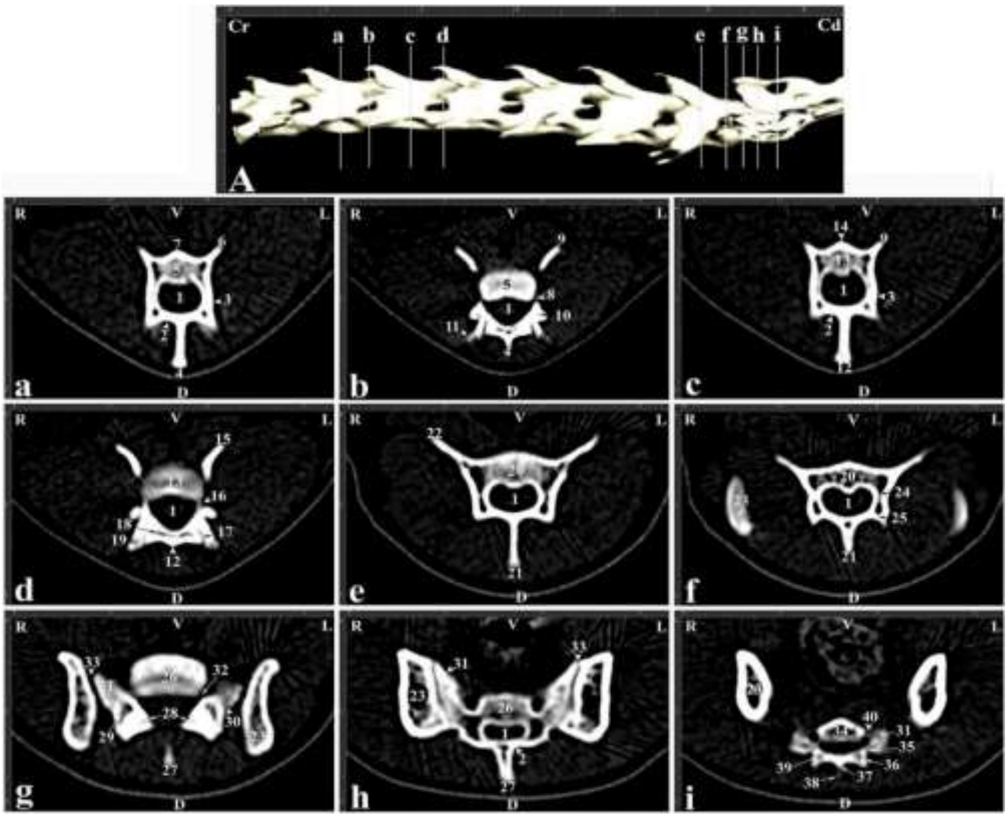

Figure 1: A. Three-dimensional reconstruction image of normal lumbosacral vertebrae of a one-year-old male guinea pig (*Cavia porcellus*) in the lateral plan. (a–d) Transverse computed tomography images related to L_1 to L_3 vertebrae and (e-i) Transverse CT images of L_6 to sacrum. (1) Vertebral foramen, (2) Vertebral lamina, (3) Vertebral pedicle, (4) Spinous process of L_1, (5) Body of L_1, (6) Transverse process of L_1, (7) Ventral crest of L_1 body, (8) Intervertebral notch of L_1, (9 Transverse process of L_2, (10) Caudal articular process of L_1, (11) Cranial articular process of L_2, (12) Spinous process of L_2, (13) Vertebral body of L_2, (14) Ventral crest of L_2 body, (15) Transverse process of L_3, (16) Intervertebral notch of L_2-L_3, (17) L_2-L_3 articular process joint, (18) Cranial articular process of L_3, (19), Caudal articular process of L_2 (20) Body of L_6, (21) Spinous process of L_6, (22) Transverse process of L_6, (23) Iliac wing, (24) Lateral recess, (25) Caudal articular process of L_6, (26) Body of S_1, (27) Spinous process of S_1, (28) Caudal articular process of L_6, (29) Cranial articular process of S_1, (30) L_6-S_1 articular process joint, (31) Sacral wing, (32) L_6-S_l intervertebral foramen, (33) Sacroiliac joint, (34) Spinous process of L_4, (35) Body of L_4, (36) Transverse process of L_5, (37) Intervertebral notch of L_4-L_5, (38) Caudal articular process of L_4, (39) Cranial articular process of L_5, (40) L_4-L_5 articular process joint. L: Left, R: Right, V: Ventral, D: Dorsal, Cr: Cranial, Ca: Caudal. The scale of the figures is in centimeters.

According to our observations, the sacrum of all guinea pigs had a triangular shape and was composed of the fusion of four vertebrae (Figure 2). The sacrum bone included a body, two wings, base and apex. The wings had an articular facet in their lateral part to articulate with the ilium. The inner surface of the wings (or a*lae*) was narrow. The bodies of the sacrum vertebrae were seen as elongated segments. The long axis of the body of each sacrum vertebra was flat and had dorsal and ventral surfaces. The dorsal surface of the body was wide on the cranial part and narrow on the caudal part. The ventral surface of the sacral body was smooth and had three transverse lines. In fact, these three transverse lines were a sign of the fusion of the four sacral vertebrae. Two transverse lines were seen on the ventral surface of the sacral body of a female guinea pig that had three vertebrae. The promontory could be recognized at the body base of the first sacral vertebra. The spinous processes of the sacrum formed of a bony plate in both males and females. The height of the spinous process of the sacrum decreased from the cranial to the caudal side. The narrow transverse processes were located on the sides of the sacrum, with a small protrusion in their caudal part. Two transverse processes were seen as small projections originating from the body of the last sacral vertebra. Therefore, the integration of the transverse processes of the sacrum did not form a plate-shaped structure in guinea pigs. There were two and three foramina on the ventral and dorsal surfaces of the sacrum, respectively. A middle and two lateral crests were visible on the dorsal surface of the sacrum. The lateral sacral crests were thin and located on the sides of the middle crest. Two cranial articular processes were distinctly recognizable, articulating with the caudal articular processes of the last lumbar vertebra. The cranial opening of the sacral spinal canal was triangular, while the caudal opening was aperture-shaped. Fusion of the sacrum bone with the last lumbar vertebra and the first coccygeal vertebra was not observed in any of the studied guinea pigs study (Figure 3).

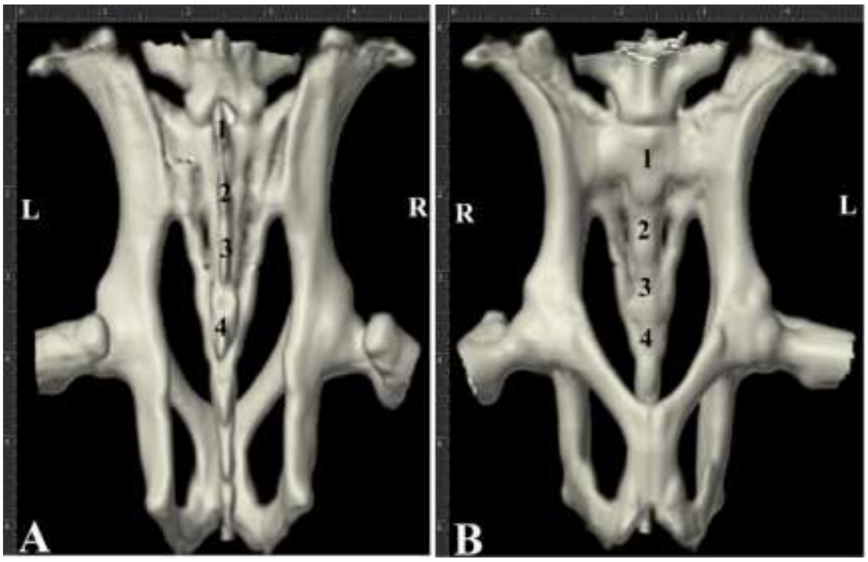

Figure 2: Dorsal (A) and ventral (B) views of the sacrum of a 12-month-old male guinea pig pig (*Cavia porcellus*). The sacrum is triangular in shape and is formed by the fusion of four vertebrae. The scale of the figures is in centimeters.

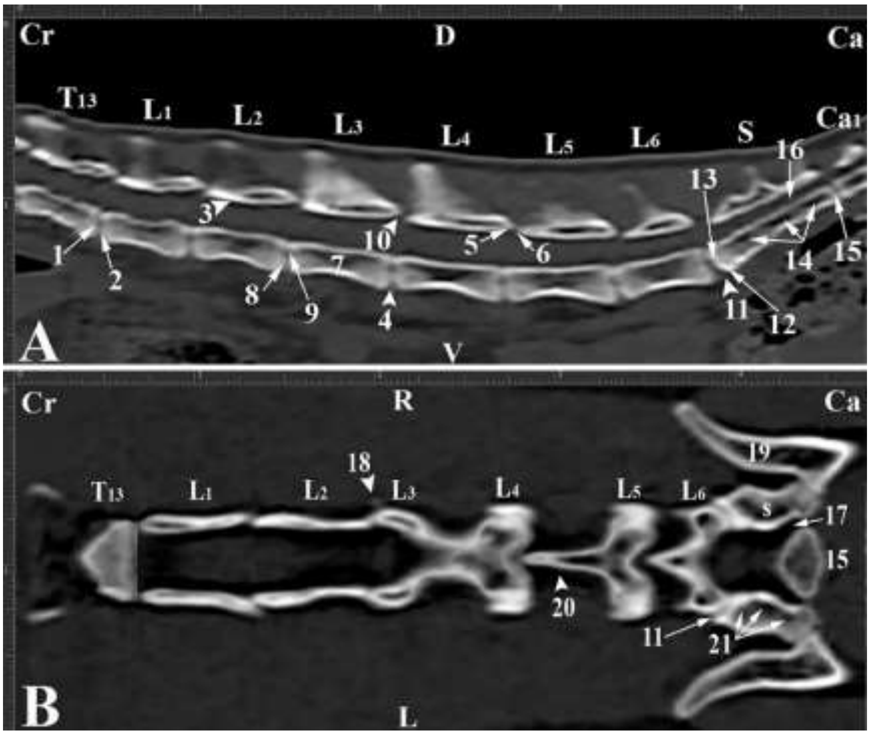

Figure 3: Sagittal (A) and dorsal (B) computed tomography reconstruction images of the lumbosacral vertebrae of a one-year-old female guinea pig (*Cavia porcellus*). (1) Caudal extremity of body T_{13}, (2) Cranial extremity of body L_1, (3) Vertebral arch, (4) Intervertebral disc of L_3 and L_4, (5) Cranial articular process of L_4, (6) Caudal articular process of L_5, (7) Body of L_3, (8) Annulus Fibrosus, (9) Nucleus Pulposus, (10) Joints of articular processes of L_3 and L_4, (11) Lumbosacral joint, (12) Promontory, (13) Base of sacrum, (14) Transverse lines, (15) Apex of sacrum, (16) Sacral canal, (17) Lumbosacral joint, (18) Mammillary process, (19) Iliac wing, (20) Spinous process of L_5, (21) Pelvic and dorsal sacral foramina of T_{13}. T_{13}: 13th thoracic vertebra, L_1: First lumbar vertebra, L_2: 2d lumbar vertebra, L_3: 3th lumbar vertebra, L_4: 4th lumbar vertebra, L_5: 5th lumbar vertebra, L_6: 6th lumbar vertebra S: Sacrum, Ca_1: The first caudal vertebra, L: Left, R: Right, V: Ventral, D: Dorsal, Cr: Cranial, Ca: Caudal. The scale of the figures is in centimeters.

In this study, morphometric measurements of different parts of the lumbosacral vertebrae were performed and subjected to statistical analysis (Tables 2 and 3). The average height of the sacrum body in male and female guinea pigs was 2.75±0.13 mm and 2.60±0.18 mm, respectively. The apex of the female guinea pigs sacrum was wider than that of males (Table 3). The BL and SPH parameters of the lumbar vertebrae were higher in males than in females, and this difference was statistically significant ($P \leq 0.05$). Other parameters of the lumbar vertebrae were greater in males than in females, but no statistically significant difference was observed between them ($P \geq 0.05$) (Table 2). The BL parameter of the sacrum bone was higher in males than in females, and the BCrW parameter was greater in females than in males, with these differences being statistically significant ($P \leq 0.05$). Other parameters of the sacrum bone were greater in males than in females, but no statistically significant difference was observed between them ($P \geq 0.05$) (Table 3).

Table 2: Statistical evaluation (Mean ± standard deviation) of variable values of Lumbar vertebrae (mm) in female and male guinea pigs (*Cavia porcellus*)

Parameters		L_1	L_2	L_3	L_4	L_5	L_6
BL	Female	7.23±0.22	8.11±0.17	8.68±0.25	8.98±0.17	8.41±0.27	7.73±0.22
	Male	7.95±0.22*	8.78±0.33*	9.46±0.23*	9.75±0.30*	9.23±0.26*	8.48±0.20*
APD	Female	9.88±0.27	10.30±0.32	10.95±0.30	11.28±0.27	11.43±0.27	11.13±0.25
	Male	10.13±0.35	10.56±0.27	11.21±0.30	11.71±0.22	11.88±0.11	11.45±0.22
AD	Female	6.48±0.22	7.35±0.32	7.26±0.27	8.11±0.30	8.35±0.30	6.51±0.30
	Male	6.63±0.30	7.48±0.20	7.45±0.20	8.30±0.32	8.53±0.35	6.66±0.27
TH	Female	6.01±0.27	6.46±0.27	8.51±0.30	9.53±0.35	8.70±0.25	9.63±0.32
	Male	6.21±0.20	6.60±0.25	8.70±0.32	9.75±0.30	8.90±0.25	9.81±0.32
BH	Female	2.53±0.12	2.18±0.17	2.61±0.20	3.10±0.15	3.23±0.17	2.70±0.18
	Male	2.63±0.07	2.31±.017	2.76±0.20	3.18±0.15	3.36±0.20	2.83±0.20
SPH	Female	1.00±0.15	1.21±0.12	1.10±0.10	1.06±0.10	1.01±0.12	0.81±0.07
	Male	1.28±0.07*	1.45±0.08*	1.40±0.05*	1.31±0.06*	1.31±0.08*	1.06±0.07*
VDCrF	Female	2.98±0.17	2.38±0.17	3.46±0.12	3.41±0.22	3.60±0.25	2.31±0.17
	Male	3.08±0.12	2.51±0.20	3.58±0.07	3.51±0.22	3.70±0.20	2.36±0.20
HDCrF	Female	4.51±0.22	4.60±0.13	4.38±0.22	4.13±0.22	4.21±0.22	4.13±0.22
	Male	4.63±0.15	4.70±0.05	4.53±0.12	4.25±0.08	4.30±0.10	4.25±0.15
VDCaF	Female	3.40±0.25	2.90±0.27	2.98±0.17	3.21±0.22	3.30±0.25	2.91±0.30
	Male	3.51±0.28	3.00±0.25	3.11±0.18	3.33±0.27	3.40±0.30	3.03±0.20
HDCaF	Female	4.61±0.32	3.51±0.25	3.13±0.22	4.41±0.30	4.40±0.25	4.10±0.25
	Male	4.71±0.32	3.63±0.20	3.26±0.22	4.53±0.30	4.50±0.25	4.18±0.25

Body length (BL), Articular processes distance (APD), Arch borders distance (AD), Total height (TH), Body height (BL), Spinous process height (SPH), Vertical diameter of cranial foramen (VDCrF), Horizontal diameter of cranial foramen (HDCrF), Vertical diameter of caudal foramen (VDCaF) and Horizontal diameter of caudal foramen (HDCaF). The significance level was set at 0.05 and the confidence limit was 95%. The significant parameters are marked with an asterisk (*).

Table 3: Statistical evaluation (Mean ± standard deviation) of variable values of Sacrum bone (in mm) in female and male guinea pigs (*Cavia porcellus*)

Parameters	Sacrum	
	Female	Male
BL	17.77±0.32*	19.91±0.25*
APD	19.25±0.62	19.53±0.55
AD	13.50±0.62	13.75±0.65
TH	9.80±0.32	9.93±0.35
BH	2.60±0.18	2.75±0.13
SPH	0.71±0.12	0.80±0.15
VDCrF	2.51±0.22	2.61±0.25
HDCrF	3.56±0.22	3.70±0.22
VDCaF	2.30±0.25	2.40±0.27
HDCaF	2.73±0.27	2.81±0.25
BCrW	16.75±0.28*	15.87±0.42*
BCaW	8.53±0.32	8.36±0.62
LSL	14.92±0.44	15.15±0.37
MSL	11.35±0.37	11.51±0.35

Body length (BL), Articular processes distance (APD), Arch borders distance (AD), Total height (TH), Body height (BH), Spinous process height (SPH), Vertical diameter of cranial foramen (VDCrF), Horizontal diameter of cranial foramen (HDCrF), Vertical diameter of caudal foramen (VDCaF), Horizontal diameter of caudal foramen (HDCaF), Body cranial width (BCrW), Body caudal width (BCaW), Lateral sacral crest length (LSL) and Medial sacral crest length (MSL). The significance level was set at 0.05. The significant parameters are marked with an asterisk (*).

Discussion

In veterinary science, different methods are used to diagnose diseases in animals (Muhamediyeva et al., 2023). Diagnostic imaging is one of these advanced methods that play an important role in the diagnosis and control of diseases. The CT is one of the most practical and accurate diagnostic imaging methods used to investigate diseases in various animals (Zhou and Liu, 2024).

Recent studies have increasingly focused on the use of the CT in animals, with most research concentrating on diagnosing skeletal diseases (Kim et al., 2024). To accurately diagnose various diseases and complications in animals using the CT scan images, it is essential to first understand the images of the normal anatomical structures of these animals. However, there are limited reports on the normal anatomy of animals based on the CT findings (Gontijo et al, 2020).

In this study, the morphological and morphometric characteristics of normal lumbosacral vertebrae of guinea pig (*Cavia porcellus*) were investigated using the CT scan images. The findings presented in this study contribute to the existing body of knowledge by providing detailed information on the normal anatomical structures of guinea pigs, which is crucial for accurate diagnosis and treatment planning.

In a retrospective study, Grosso (2019) reported the normal skeletal anatomy of exotic animals based on the CT findings. Similarly, Lauber et al, (2017) described the CT as an accurate diagnostic method for evaluating skeletal diseases and spine complications in both exotic and laboratory animals. Mitrović et al, (2023), by examining the morphology of the lumbar vertebrae in guinea pig, reported that the greatest pressure is on the L_4 vertebra. This finding is consistent with our study, which showed that the L_4 vertebra had the greatest height and depth of the spinal canal. In contrast, in humans, the greatest pressure is typically on the last lumbar vertebrae due to the axial load of the spine.

Dayan et al, (2019) presented the 3D computed tomography anatomy of the cranial and caudal limb bones of the guinea pigs in a software format. In another study, De Silva (2022) provided a comparative anatomical atlas of various guinea pig tissues based on the CT images, intended for use by researchers and veterinary clinicians. Additionally, Del Chicca et al, (2023) stated that the CT anatomy of guinea pigs serves as a diagnostic reference and plays a role in identifying different species of this animal in biometric research.

The present study investigated the CT features of the lumbosacral vertebrae in adult guinea pigs. To do this, fourteen morphometric indices of lumbosacral vertebrae were described and their various parts were identified and analyzed statistically. According to the findings, all guinea pigs had six lumbar and four sacrum vertebrae. Notably, the sacrum of a female guinea pig consisted of three fused vertebrae. These results align with Martinez-Pereira's (2021) study, which reported that the number of sacral vertebrae is not constant in most rodents.

Green (2021) by conducting an anatomical study, reported that the guinea pig sacrum consists of four fused vertebrae and features a notched crest on its spinous process. This finding contradicts our study, as our observations indicated that the spinous processes of the sacrum in both male and female guinea pigs were in the form of a bony plate without any notched crest. Additionally, Shomer et al, (2015) reported the presence of spherical accessory processes on the caudal part of the pedicles of the first to third lumbar vertebrae in guinea pigs. This observation is also inconsistent with our findings.

Our findings indicate that in both male and female guinea pigs, two lateral recesses were visible in the caudal vertebral foramina of L_6 at the junction of the pedicle and the vertebral body. This anatomical feature of guinea pig lumbar vertebrae has not been previously described in any anatomical texts and is reported for the first time in this study. Some Studies on other rodents, such as mice and rabbits, have shown that these lateral processes contain nerve roots and spinal ganglia (Börü et al, 2024). It appears that the same might be true for guinea pigs; however, specific studies are recommended to confirm this. Furthermore, the CT images obtained in the present study reveal that the range of ligaments in the lumbar region of guinea pigs can be identified as a thin soft tissue in the central part of some intervertebral discs.

Considering that magnetic resonance imaging (MRI) is preferable to CT for examining the soft tissues (Nahas et al, 2024), it is recommended to use MRI or micro CT when examining these ligaments. The transverse processes of the lumbar vertebrae in both sexes of guinea pigs were short and flat, located craniolaterally and somewhat ventrally. These findings were consistent with the study of Usha et al, (2020) but in contrast with the report by Skinner et al, (2021), which stated that the length of transverse processes is uniform across all lumbar vertebrae in rodents such as guinea pigs and rats. In our observations, L_1 and L_3 vertebrae of guinea pigs had the shortest and longest transverse processes, respectively.

Sánchez-Macías et al, (2016) reported that the length of the lumbar vertebrae body of guinea pigs is 1.5 times the length of the thoracic vertebrae body, and the length of the second thoracic vertebra body is equal to the sixth lumbar vertebra body. The first part of this report does not align with our findings, as our observations indicated that the L3 vertebra body length was longer than that of the other lumbar vertebrae. Additionally, the L_4 vertebra had the greatest height and depth of the spinal canal.

The present study found that the diameter of the intervertebral notches L_1 and L_2 was narrow, but it gradually increased up to the L_6 vertebra. This observation is consistent with the study by Sui et al, (2022). Knowledge of this anatomical feature of guinea pig lumbar vertebrae can be crucial for diagnosing inflammation and swelling of the lumbar spinal cord.

Jerome et al, (2018) through extensive anatomical studies on various rodents, reported that the articular surfaces at the extremiti es of the lumbar vertebrae bodies in guinea pigs are narrow and uneven. However, this claim contradicts the findings of the present study. Our observations revealed that the articular surfaces of the cranial and caudal extremities of the lumbar vertebrae bodies in guinea pigs were wide and smooth.

By examining the spinal formula of 240 guinea pigs in a retrospective study, Proks et al, (2015) reported that 80.4% of them had four sacral vertebrae and 82% of six lumbar vertebrae. Additionally, a lumbosacral transitional vertebra was observed in one guinea pig. These findings are not consistent with our study. According to the results, all guinea pigs under study had six lumbar vertebrae, and the sacrum was composed of four fused vertebrae. No congenital vertebral anomalies such as lumbosacral transitional vertebra, were observed in any of these animals.

Our research was conducted on guinea pigs of the *Cavia porcellus* breed, while the study by Proks et al. did not mention the breed or species of these pigs, suggesting that this discrepancy might be due to breed variations In our present study, we used 10 guinea pigs (Cavia porcellus) to examine different parts of their normal lumbosacral vertebrae based on CT scan images. It is recommended that future research include a larger sample size of guinea pigs (Cavia porcellus) to provide more detailed information on their spinal formula.

In another retrospective study, Sasai et al, (2015) reported that micro-CT has a greater diagnostic value than radiography in diagnosing pelvic fractures in rabbits. This is due to the phenomenon of tissue overlap and superimposition in radiography, whereas CT images allow for separate examination of all tissues (Sasai et al, 2015). Additional advantages of CT include providing high-resolution and three-dimensional images of animal anatomy, better differentiation of similar tissues, more accurate identification and diagnosis of cancers, and a reduced need for exploratory surgeries.

In a study, Chawla et al, (2021) reported that the spinous processes of the sacrum are triangular in guinea pigs. However, this finding is inconsistent with our observations. According to our CT images, the spinous processes of the sacrum in both sexes of guinea pigs were in the form of a bony plate and their height decreased from the cranial to the caudal side. Additionally, our observations indicated that there were two and three foramens on the ventral and dorsal surfaces of the sacrum on both sexes, respectively, which appear to be the exit sites of the dorsal and ventral sacral spinal nerves.

The anatomical differences observed in the lumbosacral vertebrae of guinea pigs, as detailed in this study, provide a basic reference for the clinicians and researchers working with this species. By establishing the normal morphology and morphometry of this region, our findings serve as a critical baseline for identifying deviations that may indicate pathological conditions, congenital anomalies, or trauma. The CT-anatomy plays a crucial role in the modern veterinary medicine, fundamentally changing how we diagnose and treat animals. It allows veterinarians to visualize the lumbosacral vertebrae of guinea pigs non-invasively, providing detailed insights into their anatomy and aiding in the diagnosis of a wide range of conditions.

In clinical practice, understanding these normal anatomical parameters allows veterinarians to more accurately interpret diagnostic imaging, such as radiographs CT scans or MRI, and differentiate between normal variations and potential abnormalities. For instance, variations in vertebral size, shape, or alignment could signal conditions like spinal deformities, degenerative diseases, or injuries. Early detection of such abnormalities can lead to more timely and targeted interventions, improving outcomes for affected animals. Furthermore, this knowledge is particularly valuable in comparative anatomy and translational research, where guinea pigs are often used as model organisms. By clarifying the normal anatomy of the lumbosacral region, our study enhances the accuracy of experimental designs and the interpretation of results in studies involving spinal health, biomechanics, or related fields. In summary, the anatomical data presented in this study directly supports the clinical interpretation and diagnosis by providing a clear standard for normal anatomy, enabling clinicians to recognize and address abnormal cases with greater confidence and precision.

One of the limitations of this research may include the small sample size of 10 healthy adult guinea pigs used in the study. While this sample size may be appropriate for a descriptive study, it may limit the generalizability of the findings to a larger population of guinea pigs. Additionally, the study focused on the normal lumbosacral vertebrae morphology and morphometrics, which may not fully capture the variability or abnormalities that could be present in diseased or injured guinea pigs.

Furthermore, the reliance of the study on the CT scan images for evaluation may have limitations in terms of resolution, image quality, and potential artifacts that could affect the accuracy of the measurements and observations made. Interpretation of the CT scan images, especially in exotic animals like guinea pigs, may also require specialized training and expertise, which could affect the reproducibility of the results. It is important for the future research in this area to consider these limitations and potentially address them through larger sample sizes, validation studies, and collaboration with veterinary professionals to ensure the clinical relevance and applicability of the findings.

This study was conducted on adult male and female guinea pigs (*Cavia porcellus*). It is hoped that the future studies will include more extensive research on immature guinea pigs and other species of guinea pigs.

The findings of this study demonstrate that the CT can provide valuable clinical information about the anatomical structures of the lumbosacral vertebrae of the guinea pig (*Cavia porcellus*), information that is not attainable with conventional diagnostic imaging methods. Additionally, evaluating the tomographic characteristics of the lumbosacral vertebrae in this species can aid in identifying the anatomical features and assessing pathological complications. In this study, images with acceptable resolution of the details of different parts of the lumbosacral vertebrae of guinea pigs (*Cavia porcellus*) were obtained by employing the appropriate radiation factors and suitable windows.

The results of the current study allow the clinicians to detect abnormalities such as herniated discs, spinal tumors, lumbar spinal stenosis, fractures, and the other injuries that may not be visible on other imaging tests. These findings could also help screen guinea pigs with back and leg pain who do not have neurological deficits. It may determine the need for further studies, such as myelography. The results of this study revealed that the CT can easily detect disorders related to the lumbosacral vertebrae canal in guinea pigs. The CT allows for the investigation of articular process joints, sacroiliac joints, intervertebral foramina and dorsal sacral foramina without superimposition. According to our findings, the interarcuate spaces of guinea pig lumbar vertebrae were very narrow, but this space was wide and large between the L_6 and S_s vertebrae. Therefore, for epidural anesthesia, surgeons can perform cerebrospinal fluid puncture and administer anesthetic drugs at this location.

The results of this research can be applied in teaching the CT anatomy of lumbosacral vertebrae, interpretation of the CT scan images, as well as in clinical and treatment decisions of guinea pig (*Cavia porcellus*).

Ethical Consideration

Approval for the study was granted by the Ethical Review Committee at the Islamic Azad University of Urmia Branch, Iran (Approval Number: IR.IAU.URMIA.REC.1403.129), ensuring compliance with ethical codes for research on animals. The experiment was supervised by the Iranian Society for Prevention of Cruelty to Animals, underscoring the commitment to humane treatment throughout the study.

Acknowledgments

The authors thank the Vice Chancellor for Research of Islamic Azad University of Urmia for their financial supports (Protocol Code: 4/ 39822). This article is the outcome of DVM student thesis.

Conflict of Interest

The authors declare that they have no conflict of interest.

Funding

This research was carried out in the form of a thesis with the financial support of Islamic Azad University of Urmia.

References

Barbera, A. M., Delaunay, M. G., Dougill, G., & Grant, R. A. (2019). Paw morphology in the domestic guinea pig (Cavia porcellus) and brown rat (Rattus norvegicus). *The Anatomical Record*, *302*(12), 2300-2310.

Boonsri, B., Buddhachat, K., Punyapornwithaya, V., Phatsara, M., & Nganvongpanit, K. (2020). Determination of whether morphometric analysis of vertebrae in the domestic cat (Felis catus) is related to sex or skull shape. *Anatomical Science International*, *95*, 387-398.

Boonsri, B., Nganvongpanit, K., Buddhachat, K., Punyapornwithaya, V., Kongtueng, P., Kaewmong, P., & Kittiwattanawong, K. (2021). Morphometric analysis of cervical vertebrae in some marine and land mammals. *Anatomia, histologia, embryologia, 50*(5), 812-825.

Börü, Ü. T., Sarıtaş, Z. K., Özbek, F. G., Bölük, C., Acar, H., Koç, Y., & Demiral, G. Z. (2024). Alterations in the spinal cord, trigeminal nerve ganglion, and infraorbital nerve through inducing compression of the dorsal horn region at the upper cervical cord in trigeminal neuralgia. *Brain Research, 1832*, 148842.

Bouxsein, M. L., Boyd, S. K., Christiansen, B. A., Guldberg, R. E., Jepsen, K. J., & Müller, R. (2010). Guidelines for assessment of bone microstructure in rodents using micro–computed tomography. *Journal of bone and mineral research, 25*(7), 1468-1486.

Carrera, A. C., Moreno, I. F., Celoto, M. G., Sprada, A. G., Requena, R., Jassniker, J. B., & Paula, C. G. (2022). Retrospective study on the incidence of cats and dogs' spinal injuries by computed tomographic scan. Part II: Thoracolumbar and lumbosacral. *Rev. bras. ciênc. vet*, 27-35.

Chawla, S., Jena, S., & Nayak, S. (2021). The Laboratory Guinea Pig. *Essentials of Laboratory Animal Science: Principles and Practices*, 239-251.

Da Costa, R. C., & Samii, V. F. (2010). Advanced imaging of the spine in small animals. *Veterinary Clinics: Small Animal Practice, 40*(5), 765-790.

Dayan, M. O., Beşoluk, K., Eken, E., Aydoğdu, S., & Turgut, N. (2019). Three-dimensional modelling of the femur and humerus in adult male guinea pigs (guinea pig) with computed tomography and some biometric measurement values. *Folia Morphologica*, *78*(3), 588-594.

De Silva, M. (2022). Gross and Microscopic Morphological Anatomical Study of the Guinea Pig (Cavia porcellus) and the Capybara (Hydrochoerus hydrochaeris), Aimed at the Preparation of a Comparative Anatomical Atlas of the Different Systems.

Del Chicca, F., Puccinelli, C., Petrini, D., & Citi, S. (2023). Incidental Findings in Computed Tomography Examination of the Head in Rabbits and Guinea Pigs. *Veterinary Sciences*, *10*(8), 504.

Gontijo, R. M. G., Ferreira, A. V., Silva, J. B., & Mamede, M. (2020). Quality control of small animal PET scanner: The Brazilian Scenario. *Brazilian Journal of Radiation Sciences, 8*(2).

Green, K. (2021). Using acupuncture to manage wound healing and chronic back pain in a guinea pig. *Companion Animal, 26*(9), 1-10.

Grosso, F. V. (2019). Orthopedic diagnostic imaging in exotic pets. *Veterinary Clinics: Exotic Animal Practice*, *22*(2), 149-173.

Jerome, C., Hoch, B., & Carlson, C. S. (2018). Skeletal system. In *Comparative anatomy and histology* (pp. 67-88): Elsevier.

Kim, S., Jang, S., & Lee, O. (2024). Simultaneous visualization of micro-damage in cortical bone, trabecular bone, and intracortical vasculature for diagnosing osteoporosis: An animal model synchrotron imaging. *Microscopy Research and Technique*, *87*(4), 695-704.

Lauber, D. T., Fülöp, A., Kovács, T., Szigeti, K., Máthé, D., & Szijártó, A. (2017). State of the art in vivo imaging techniques for laboratory animals. *Laboratory animals*, *51*(5), 465-478.

Liau, Z. Q. G., Lam, R. W. M., Hu, T., & Wong, H.-K. (2017). Dose-dependent nerve inflammatory response to rhBMP-2 in a rodent spinal nerve model. *Spine*, *42*(16), E933-E938.

Mähler, M., Berard, M., Feinstein, R., Gallagher, A., & Raspa, M. (2014). FELASA recommendations for the health monitoring of mouse, rat, hamster, guinea pig and rabbit colonies in breeding and experimental units. *Laboratory animals*, *48*(3), 178-192.

Martinez-Pereira, M. A. (2021). Comparative anatomy of the lumbosacral plexus. In *Surgical anatomy of the sacral plexus and its branches* (pp. 189-204): Elsevier.

Martz, E. O., Goel, V. K., Pope, M. H., & Park, J. B. (1997). Materials and design of spinal implants—a review. *Journal of Biomedical Materials Research, 38*(3), 267-288.

McDougall, J. J., Andruski, B., Schuelert, N., Hallgrímsson, B., & Matyas, J. R. (2009). Unravelling the relationship between age, nociception and joint destruction in naturally occurring osteoarthritis of Dunkin Hartley guinea pigs. *PAIN®, 141*(3), 222-232.

Mitrović, M. J., Kitanović, S., Tatalović, N., Todorović, A., & Macanović, M. L. (2023). Radiological Investigation of Guinea Pig () Lumbar Vertebral Morphology–A Biomechanical Aspect. *Acta Veterinaria, 73*(1), 55-70.

Moarabi, A., Ghadiri, A., Mosallanejad, B., & Koochak, M. (2024). Radiographic evaluation of bone disorders in referred dogs to Veterinary Hospital of Shahid Chamran University of Ahvaz. *Iranian Veterinary Journal, 20*(3), 76-86.

Muhamediyeva, D., Safarova, L., & Tukhtamurodov, N. (2023). *Early diagnostics of animal diseases on the basis of modern information technologies.* Paper presented at the AIP Conference Proceedings.

Munif, M. R., Safawat, M. S., & Hannan, A. (2023). Surgical intervention for the correction of fecal impaction in an obstipated cat with an old compression injury in the lumbosacral region of the spine. *Bulletin of the National Research Centre, 47*(1), 133.

Nahas, A. E., Almohamad, Z., & Hagag, U. (2024). Ultrasonography, computed tomography and magnetic resonance imaging of the dromedary camel distal limbs. *BMC veterinary research, 20*(1), 12.

Özkadif, S., Eken, E., Beşoluk, K., & Dayan, M. (2015). Three-dimensional reconstruction of New Zealand rabbit antebrachium by multidetector computed tomography. *Iranian journal of veterinary research, 16*(2), 205.

Pignon, C., & Mayer, J. (2020). Guinea pigs. Ferrets, Rabbits, and Rodents: Clinical Medicine and Surgery. *Elsevier*, 270-97.

Proks, P., Johansen, T. M., Nývltová, I., Komenda, D., Černochová, H., & Vignoli, M. (2021). Vertebral formulae and congenital vertebral anomalies in guinea pigs: A Retrospective Radiographic Study. *Animals, 11*(3), 589.

Proks, P., Stehlik, L., Paninarova, M., Irova, K., Hauptman, K., & Jekl, V. (2015). Congenital abnormalities of the vertebral column in ferrets. *Veterinary Radiology & Ultrasound, 56*(2), 117-123.

Sánchez-Macías, D., Castro, N., Rivero, M. A., Argüello, A., & Morales-delaNuez, A. (2016). Proposal for standard methods and procedure for guinea pig carcass evaluation, jointing and tissue separation. *Journal of Applied Animal Research, 44*(1), 65-70.

Sasai, H., Fujita, D., Tagami, Y., Seto, E., & Hamakita, H. (2015). Characteristics of bone fractures and usefulness of micro–computed tomography for fracture detection in rabbits: 210 cases (2007–2013). *Journal of the American Veterinary Medical Association*, *246*(12), 1339-44.

Segal, U., Bar, H., & Shani, J. (2018). Repair of lumbosacral fracture–luxation with bilateral twisted string-of-pearls locking plates. *Journal of Small Animal Practice, 59*(8), 501-507.

Shomer, N. H., Holcombe, H., & Harkness, J. E. (2015). Biology and diseases of guinea pigs. In *Laboratory animal medicine* (pp. 247-283): Elsevier.

Skinner, Z., Clark, N., Rutland, S., Dawkins, A., & Rutland, C. S. (2021). Skeleton growth in guinea pigs and humans. *Frontiers for Young Minds, 9*.

Soroori, S., Zehtabvar, O., Shateri-Amiri, B., Rostami, A., & Vali, Y. (2022). Computed Tomographic and Morphometric Study of Lumbosacral and Coccygeal Vertebrae in Healthy White New Zealand Rabbit (Oryctolagus Cuniculus). *Iranian Journal of Veterinary Surgery*.

Sui, J., Jin, M., Morovvati, H., & Goorani, S. (2022). Local anesthetic, anti-inflammatory and analgesic activities of nanoparticles green-formulated by plant extract. *Inorganic Chemistry Communications, 143*, 109642.

Sun, Y., Helmholz, H., & Willumeit-Römer, R. (2022). Surgical classification for preclinical rat femoral bone defect model: standardization based on systematic review, anatomical analysis and virtual surgery. *Bioengineering, 9*(9), 476.

Usha Kumary, S., Sathya Moorthy, O., Raja, K., & Ramesh, G. (2020). Gross Anatomical Observations on the Sacrum of Guinea Pig (Cavia porcellus).

Veterinaria, N. A. (2017). International committee on veterinary gross anatomical nomenclature (ICVGAN). Published by the Editorial Committee, Hannover.

Wilhite, R., & Wölfel, I. (2019). 3D Printing for veterinary anatomy: An overview. *Anatomia, histologia, embryologia, 48*(6), 609-620.

Wills, D. J., Neville-Towle, J., Podadera, J., & Johnson, K. A. (2022). Computed tomographic evaluation of the accuracy of minimally invasive sacroiliac screw fixation in cats. *Veterinary and Comparative Orthopaedics and Traumatology*, *35*(02), 119-127.

Witkowska, A., Alibhai, A., Hughes, C., Price, J., Klisch, K., Sturrock, C. J., & Rutland, C. S. (2014). Computed tomography analysis of guinea pig bone: architecture, bone thickness and dimensions throughout development. *PeerJ*, *2*, e615.

Zhou, X., & Liu, Z. (2024). Computerized tomography. In *Computational Optical Imaging: Principle and Technology* (pp. 101-134): Springer.

Zipser, B., Schleking, A., Kaiser, S., & Sachser, N. (2014). Effects of domestication on biobehavioural profiles: a comparison of domestic guinea pigs and wild cavies from early to late adolescence. Frontiers in zoology, 11(1):1-14.

Received: 11.10.2024
Accepted: 14.04.2025

مقاله کامل

دوره بیست و یکم ـ شماره ۱ ـ بهار ۱۴۰۴

DOI: 10.22055/ivj.2025.482863.2744

مطالعه مورفولوژی و مورفومتری مهره‌های کمری خاجی در خوکچه هندی (*Cavia porcellus*) بر اساس تصاویر سی‌تی اسکن

الهه گلی[۱]، سیامک علیزاده[۲]* و محمدرضا حسینچی[۳]

[۱] دانش‌آموخته دکترای حرفه‌ای دامپزشکی، دانشکده دامپزشکی، واحد ارومیه، دانشگاه آزاد اسلامی، ارومیه، ایران

[۲] استادیار گروه علوم درمانگاهی، دانشکده دامپزشکی، واحد نقده، دانشگاه آزاد اسلامی، نقده، ایران

[۳] استادیار گروه علوم پایه، دانشکده دامپزشکی، واحد ارومیه، دانشگاه آزاد اسلامی، ارومیه، ایران

تاریخ دریافت: ۱۴۰۳/۷/۲۰ تاریخ پذیرش: ۱۴۰۴/۱/۲۵

چکیده

توموگرافی کامپیوتری (CT) از تکنیک‌های تصویربرداری تشخیصی دقیقی می‌باشد که برای ارزیابی ستون مهره‌ها در دام‌های کوچک و حیوانات اگزوتیک استفاده می‌شود. هدف از این مطالعه بررسی مورفولوژیک و مورفومتریک مهره‌های کمری خاجی نرمال در خوکچه‌هندی (*Cavia porcellus*) بر اساس تصاویر سی‌تی اسکن بود. در این مطالعه توصیفی – مقطعی از ۱۰ خوکچه‌هندی بالغ سالم (۵ نر و ۵ ماده) با میانگین سنی ۱/۲۰±۱۲ ماه و میانگین وزنی ۰/۱۵ ± ۱/۰۴ کیلوگرم استفاده شد. متعاقب بی‌هوشی خوکچه‌هندی با کوکتل داروهای زایلازین (۴ mg/kg) و کتامین (۶۰ mg/kg)، سی‌تی اسکن از مهره‌های کمری خاجی آن در پلن‌های ساجیتال، عرضی و دورسال از قسمت قدامی اولین مهره کمری تا انتهای خلفی خاجی انجام گرفت. براساس نتایج این مطالعه تمامی قسمت‌های مهره‌های کمری خاجی و مفاصل بین مهره‌ای خوکچه‌هندی در تصاویر توموگرافی کامپیوتری قابل مشاهده و ارزیابی هستند. زوائد شوکی مهره‌های کمری در پلن ساجیتال و زوائد مفصلی قدامی و خلفی در بازسازی‌های ساجیتال و عرضی بهتر قابل شناسایی هستند. زوائد پستانی و شیارهای مهره‌ای قدامی و خلفی در پلن دورسال بهتر دیده می‌شوند. دو فرورفتگی جانبی در سوراخ مهره‌ای کودال L_6 در محل اتصال پدیکول و بدنه مهره قابل مشاهده بود که این ویژگی آناتومیکی برای اولین بار گزارش می‌شود. فضاهای بین کمانی (interarcuate spaces) در مهره‌های کمری خوکچه‌هندی بسیار باریک بودند، اما این فضا بین مهره‌های L_6 و S_1 پهن و بزرگ بود، لذا جراحان برای بی‌حسی اپیدورال می‌توانند از این محل نسبت به پونکسیون مایع مغزی نخاعی و تزریق داروهای بی‌هوشی اقدام نمایند. در این مطالعه اندازه‌گیری‌های مورفومتریک از قسمت‌های مختلف تشکیل دهنده مهره‌های کمری خاجی انجام یافته و تحت آنالیز آماری قرار گرفتند. نتایج این مطالعه می‌تواند برای آموزش علوم آناتومی توموگرافی کامپیوتری مهره‌های لومبوساکرال، تفسیر تصاویر CT اسکن و نیز در معاینات بالینی و امور درمانی خوکچه‌هندی (*Cavia porcellus*) مورد استفاده قرار گیرند.

کلمات کلیدی: موفولوژی، مورفومتری، خوکچه‌هندی (*Cavia porcellus*)، توموگرافی کامپیوتری، مهره‌های کمری خاجی

* نویسنده مسئول: سیامک علیزاده، استادیار گروه علوم درمانگاهی، دانشکده دامپزشکی، واحد نقده، دانشگاه آزاد اسلامی، نقده، ایران

E-mail: si.alizadeh@iau.ac.ir

© 2020 by the authors. Licensee SCU, Ahvaz, Iran. This article is an open access article distributed under the terms and conditions of the Creative Commons Attribution-NonCommercial 4.0 International (CC BY-NC 4.0 license) (http://creativecommons.org/licenses/by-nc/4.0/).